Study of Heat Transfer through Porous Fin Subjected to Periodic Base Temperature

Thesis Submitted in Partial Fulfillment of the Requirements for the Degree of

Master of Engineering in Mechanical Engineering

By

ROHIT ROY

[Examination Roll No: M4MEC24004]

[University Registration No: 163706 of 2022-2023]

Under the Guidance of

Prof. BALARAM KUNDU

DEPARTMENT OF MECHANICAL ENGINEERING

FACULTY OF ENGINEERING & TECHNOLOGY

JADAVPUR UNIVERSITY

KOLKATA – 700032

JULY 2024

FACULTY OF ENGINEERING AND TECHNOLOGY

JADAVPUR UNIVERSITY

CERTIFICATE OF APPROVAL*

This foregoing thesis is now approved as a credible study of an engineering subject carried out and presented satisfactorily to warrant its acceptance as a prerequisite to the degree for which it has been submitted. It is understood that by this approval, the undersigned does not endorse or approve any statement made, opinion expressed, or conclusion drawn therein but approves the thesis only for its submitted purpose.

COMMITTEE ----------

ON FINAL EXAMINATION FOR

EVALUATION OF THE THESIS ----------

***Only in case the thesis is approved**

FACULTY OF ENGINEERING AND TECHNOLOGY

JADAVPUR UNIVERSITY

CERTIFICATE OF RECOMMENDATION

I hereby recommend that the thesis presented under my supervision by ***Mr. ROHIT ROY*** *entitled* ***"Study of Heat Transfer through Porous Fin Subjected to Periodic Base Temperature"*** *be accepted in partial fulfillment of the requirements for the* ***Master of Engineering degree in Mechanical Engineering****.*

Thesis Supervisor

Countersigned

Head of the Department
Department of Mechanical Engineering

Dean
Faculty of Engineering and Technology

DECLARATION OF ORIGINALITY AND COMPLIANCE OF ACADEMIC ETHICS

I hereby declare that the thesis contains literature survey and original research work by the undersigned candidate, as a part of his ***MASTER OF ENGINEERING IN MECHANICAL ENGINEERING*** studies. All information in this document have been obtained and presented in accordance with the academic rules and ethical conduct.

I also declare that, as required by these rules of conduct, I have fully cited and referenced all the material and results that are not original to this work.

Name: **ROHIT ROY**

Examination Roll Number: **M4MEC24004**

Class Roll Number: **002211202009**

University Registration No: **163706 of 2022-2023**

Thesis Title: ***Study of Heat Transfer Through Porous Fin Subjected to Periodic Base Temperature***

Signature with Date:

ACKNOWLEDGEMENT

I am grateful to my advisor, Dr. Balaram Kundu, for his continuous support, expert guidance, and invaluable insights throughout this research. His encouragement and mentorship have been pivotal in the successful completion of this thesis. I also want to extend my heartfelt thanks to my friends for their camaraderie, support, and the many engaging discussions that have significantly enriched my research journey. Furthermore, I am profoundly thankful to my family for their unconditional love, patience, and faith in me, which have been a constant source of motivation and strength. Their collective contributions have been indispensable, and I am sincerely appreciative towards their support throughout the period.

Date:

(ROHIT ROY)

List of Symbols

Symbols

g	Gravitational acceleration
ρ	Density
K	Permeability
β	Volumetric thermal expansion coefficient
w	Width of fin
L	Length of fin
t_b	Fin thickness
γ	Angle of pores
T	Temperature
v	Kinematic viscosity
X	Dimensionless length
ΔX	Special step size
θ	Dimensionless temperature
τ	Dimensionless time
$\Delta\tau$	Time step size
k	Thermal conductivity
h	Heat transfer coefficient
q_{gen}	Volumetric heat generation
c_p	Specific heat

t	Time
φ	Porosity
μ	Dynamic Viscosity
α , ω, ζ_1, ζ_2, A , B, C, ξ, ψ	Arbitrary constants

Subscripts

f	Fluid
nf	Nanofluid
b	Base
bm	Base mean
a	Ambient
eff	Effective
j	Special node

Superscripts

n	Time node

List of Figures

List of Tables

Table of Contents

Abstract

This thesis presents a comprehensive heat transfer analysis of a porous fin containing nanofluid flow within its pores. The study considers a time-dependent, periodically varying base temperature at the fin. A numerical model has been developed using the finite difference method, employing the explicit Forward Time Central Space (FTCS) scheme to solve the governing equations. To validate the numerical model under time-dependent boundary conditions, an analytical solution using the Laplace transformation method was derived, which neglects nonlinear terms. Further validation for the nonlinear terms was achieved using the Adomian Decomposition Method (ADM) under the assumption of steady-state conditions with a constant base temperature. The combined analytical approaches provide a robust validation framework for the complex heat transfer mechanisms within the porous fin system, contributing valuable insights into the thermal performance of nanofluid-impregnated porous structures. Additionally, a numerical analysis was performed to determine the fin's heat transfer rate and efficiency under time-dependent boundary conditions, and we also analyzed the impact of nanofluid on the heat transfer and efficiency of the fin.

Chapter-1

1. INTRODUCTION

Efficient heat transfer is the most crucial thing in thermal engineering applications. In industrial applications, we must remove a large amount of heat from the system to avoid any thermal damage due to the development of excessive temperature or thermal stress and ensure the proper and seamless functioning of those costly gadgets. In mechanical devices that operate on cycles, such as engines and power plants, it is necessary to remove heat from the high-temperature fluid to complete the cycle. On the other hand, high-end electronic gadgets require rapid cooling technology in a compact format to accommodate the space limitation of those devices. Heat transfer augmentation has always been an essential concern for thermal engineers in real-life scenarios. For this reason, the history of heat transfer augmentation is full of scientific research proposals and engineering innovations.

Sir Isaac Newton proposed the formulation of **Newton's Law of cooling** in which he described the rate at which an object gets cooled or heated through heat transfer with its surroundings. The formula is given by

$$\frac{dQ}{dt} = hA(T - T_S)$$

Where $\frac{dQ}{dt}$ is the rate of heat transfer, h is convective heat transfer coefficient, A is surface area of the body, T is temperature of the body and T_S is surrounding temperature.

Joseph Fourier introduced the mathematical formulation for heat conduction through a solid known as **Fourier's Law of Conduction**. The law states that heat transfer rate per unit area or heat flux through a solid body is directly proportional to the negative temperature gradient in the direction of heat flow. Mathematically, it is expressed as:

$$q = -k\nabla T$$

Where q is heat flux, k is thermal conductivity of the material and ∇T is temperature gradient. These two laws are the most fundamental laws of heat transfer which have provided the groundwork for subsequent developments in the field of thermal design.

1.1 Problem description

Fast cooling is required in many real-world situations to enhance device efficiency and protect against thermal damage. Fins are commonly utilized to improve heat transfer effectiveness in such systems. In many practical scenarios, fins are subjected to varying base temperatures, such as car engines, electronic gadgets, power plant components, HVAC systems, and aerospace mechanisms.

Car engines: Effective cooling in automobile engines is crucial for preserving efficiency and avoiding overheating. In automobile engines, fins are utilized for cooling. The engine operates on a continuous 4-stroke cycle of suction, compression, power, and exhaust strokes. During each phase, the temperature of the engine walls fluctuates. Fins attached to the engine blocks are thus subjected to these varying base temperatures.

Electronic Devices: Current electronic components like CPUs and GPUs produce significant amounts of heat while in use. Effective cooling strategies are needed to prevent hardware damage. Varying computational loads cause rapid changes in the base temperature of cooling fins in those devices.

Components of power plants: Power plant components such as turbines and heat exchangers undergo fluctuating thermal loads while operating. Effective heat transfer is essential to preserve peak performance and avoid material deterioration caused by elevated temperatures.

Much research on fins assumes a constant base temperature due to the difficulty of solving PDEs with time-dependent boundary conditions despite the practical need for such analysis. Yet, tackling boundary conditions that vary with time can be very beneficial, leading to a more

thorough examination that encompasses the fixed base temperature as a specific instance of the broader solution.

Using porous fins and nanofluid flow offers an excellent solution to enhance heat transfer in these critical applications. These advanced methods can significantly improve cooling efficiency and overall performance, making them highly valuable in scenarios where fast and effective heat dissipation is crucial.

Mathematical Background:

French mathematician Pierre-Simon Laplace introduced a mathematical technique known as the Laplace Transformation Method to solve partial differential equations by transforming the time domain into the frequency domain, which converts the partial differential equation into a simple ordinary differential equation and then solves that ordinary differential equation and finally transforms back into the time domain by performing inverse Laplace operation. This technique is one of the most powerful tools in mathematics for dealing with complex mathematical models. However, the method used in this technique was the inverse Laplace operation. Augustin-Louis Cauchy did some significant research in the field of complex mathematics, and he proposed Cauchy's Integral Theorem, Cauchy's Integral Formula, and Cauchy's Residue Theorem to deal with complex integrations, which became helpful tools for Laplace inversion operation. George Adomian developed a formula to deal with nonlinear differential equations by decomposing the nonlinear term into a polynomial known as the Adomian Decomposition Method. This method can only provide a rapidly converged solution by considering a few terms in the polynomial series. In the latter part of the 20th century, computer technology improvements transformed how complex heat transfer problems were tackled. The development of numerical methods, including the finite difference method, finite volume method, and finite element method, played a crucial role. With the advent of high-performance computers, the precision of numerical solutions increased while computation times decreased, making it possible to effectively address a wide range of intricate and practical heat transfer issues. These mathematical developments significantly enhanced the accuracy of heat

transfer and fins' performance analysis, making fins suitable for complex modern applications.

1.2 Literature Review

1.2.1 Some early works

Early research on fins was predominantly focused on material and geometrical modifications to enhance the performance of fins. Harper and Brown [1] proposed an analytical solution for a 2-dimensional heat transfer model for rectangular fin, waged fin, and annular fin of constant thickness. The solution gave an expression to determine the fin efficiency. Gardner [2] derived a general expression of temperature for a fin whose thickness varies with some power of length. Horatio Scott Carslaw and John Conrad Jaeger described the theoretical aspects of heat transfer in their book Conduction of Heat in Solid [3]. This book is one of the fundamental books on heat transfer. Cobble did the first analysis of fin heat transfer by considering the combined effect of convection and radiation [4]. He analytically solved the nonlinear differential equation through a numerical approximation of the nonlinear term. His work closely matched with experimental data. Cobble [5] tried to find the best geometry through his research. He developed a steady-state nonlinear differential equation for temperature distribution and then divided the expression with half-fin length and total fin volume. The optimization process minimizes fin volume by adjusting temperature distribution parameters, yielding minimum volume designs. Ozisik [6] described various techniques to solve differential equations, such as separation of variables, Laplace transformation, etc., for various boundary conditions in his book. He solved a wide range of practical examples in his book. This book serves as a foundational framework for advancing studies in heat conduction. Minkler and Rouleau [7] analyzed a rectangular fin by considering volumetric heat generation inside the fin. Chen and Fluker [8] performed an analysis of a composite fin. They took a radial fin of two materials and solved the governing differential equation using the Laplace transformation method. They also compared the results with the fins made of a single material and found that composite fins can enhance heat transfer. Heaslet and Lomax [9] observed that thermal

conductivity varies as temperature changes, so they took thermal conductivity as a function of temperature and performed the analysis for the extended surface. They solved the nonlinear governing equation using a numerical technique.

1.2.2 Numerical Works

Cumo, Lopez, and Pinchera [10] performed the first numerical solution of an extended surface. They calculated a fin's heat transfer rate and efficiency by numerical technique. Hung and Appl [11] numerically solved the governing equation of fin by considering variable thermal conductivity, heat transfer coefficient, and thermal emissivity. Their work addressed one of the most general cases of fin heat transfer. Sane and Sukhatme [12] numerically analyzed short fins under natural convection heat transfer. They calculated the natural convective heat transfer for a horizontal fin array. They also determined the effect of various parameters in fin heat transfer. Their result closely aligned with the experimental data. Campo [13] solved the fin heat transfer equation for both steady and transient cases by considering convection and radiation. He solved the partial differential equation by the finite difference method. This was one of the earliest works on the finite difference method applied to fins. This work introduced a new approach to solving the fin heat transfer equation. Sparrow and Hsu [14] determined the convective heat transfer coefficient at the fin tip by considering the entire fin is exposed to adiabatic surroundings. They used the finite difference method to solve the governing equation. Char and Chen [15] applied the finite difference method to solve the governing equation of a two-dimensional trapezoidal fin. They performed transient analysis and determined the heat transfer through the fin surface.

1.2.3 Studies on Periodic Base Temperature

Researchers observe that in many practical case scenarios, like in automobile engines, the base temperature of a fin also varies with time. For this type of case, an unsteady state analysis was required. Chapman [16] performed a transient analysis for a radial fin subjected to a sudden stepped increase in base temperature. He solved three types of Bessel functions using the graphical method. Donaldson and Shouman [17] performed a transient analysis of a rectangular fin exposed to the environment under

starting conditions. Bertz [18] obtained a solution for radial fins of varying thickness exposed to periodic base temperature. He performed analytical solutions by Fourier transformation. After one year, Newhouse [19] also performed a similar kind of analysis but with a constant thickness radial fin exposed to periodic base temperature. Malikov [20] analyzed a two-dimensional circular fin subjected to temperature variation in radial and circumferential direction. He also considered periodic base temperature in his analysis. Sparrow and Hennecke [21] studied the temperature profile of a rectangular fin subjected to decreasing base temperature. They thought of the constant thermal conductivity of the material in their study. Yang [22] analyzed rectangular fins subjected to periodic boundary conditions. He solved the steady part and oscillating part individually and then obtained the complete solution of the governing equation analytically by superimposition. He also calculated time-averaged efficiency for a rectangular fin exposed to periodic boundary conditions. He also studied the effect of various parameters on heat transfer in his analysis. Aziz [23] performed a similar analysis for radial fin. Sparrow and Lee [24] analytically solved the heat equation for periodic base temperature by separating variables for a finned tube wall. Aziz and Na [25] solved the heat equation for periodic base temperature by a perturbation method. They also considered the effect of radiation heat transfer in their analysis. Al Mujahid [26] solved the heat equation for periodic base temperature in a triangular fin by numerical techniques.

1.2.4 Recent Advancements and Background of Porous Fin and Nanofluids

In the quest to enhance heat transfer from fins, researchers experimented with various innovative approaches. They observed that a fin's heat transfer rate directly depends on its surface area. Therefore, increasing the surface area could enhance the heat transfer rate. As a result, they developed fins made of porous materials. Darcy conducted numerous experiments on water flow through sand and documented the behavior of fluid flow and heat transfer characteristics through porous media in his book [27] Les fontaines publiques de la ville de Dijon, which became a foundational text for understanding heat transfer through porous materials. Donald A. Nield and Adrian Bejan described the principles and applications of convection

in porous materials in their book [28] "Convection in Porous Media." It covered fundamental concepts like Darcy's law, heat, mass transfer, and different types of convection. The book included mathematical models and experimental methods, making it essential for researchers and engineers. M. Kaviany described various numerical methods for solving single-phase and multiphase flow through a porous medium in his book [29] "Principles of Heat Transfer in Porous Media." S. Y. Kim and Assoc. Mem [30] performed an experimental study that explored the influence of porous fins on pressure drop and heat transfer in plate-fin heat exchangers. They performed the experiment with 6101 aluminium-alloy foam fins of varying permeabilities and porosities, revealing similar thermal performance to conventional fins but with slightly higher pressure drops. They observed the designs with high pore density and low porosity are the most effective. In 2011, Blaram Kundu and Dipankar Bhanja [31] performed a steady-state analytical solution of porous fin heat transfer. They used the domain decomposition method to deal with the non-linearity of the governing equation. Using differential transformation and finite difference methods, Sobamowo et al. [32] examined heat transfer in a moving rectangular porous fin with temperature-dependent thermal conductivity and internal heat generation. Their studies indicated increased porosity and convection enhanced heat transfer and efficiency, whereas higher thermal conductivity and internal heat generation decreased heat transfer. Recent advancements in nanofluid research have revealed promising possibilities for enhancing heat transfer in porous fins. Researchers have noted significant improvements in heat transfer when nanofluids flow through the pores of the fins. Mohammad Ghazvini and Hossein Shokouhmand [33]analyzed CuO-water nanofluids in microchannel heat sinks using analytical and numerical methods, comparing the Fin model and porous media approach. They investigated the impact of particle volume fraction, Brownian motion, channel aspect ratios, and porosities on temperature distribution, heat transfer, and friction factor and identified an optimal aspect ratio. Sowmya, Gireesha, and Prasannakumara [34] investigated the thermal behavior of radial porous fins wetted with nanofluids containing molybdenum disulfide nanoparticles in water. They explored non-spherical nanoparticle shapes such as platelets, cylinders, bricks, and blades. They solved the governing equation numerically using the Runge Kutta Fehlberg method and found that brick-shaped nanoparticles are the most effective among those

examined. Manohar et al. [35] described that semi-spherical fins have been widely valued for their efficient thermal exchange properties, commonly applied in aerospace, chemical processing, and electronics. They studied the performance of hybrid nanofluids over these fins using Darcy's model. It examined internal heat generation, natural convection, and radiation effects, analyzing their specific influences on fin surface temperatures through numerical methods. Baslem et al. [36] analyzed heat transfer through a fully wetted longitudinal permeable fin using nano liquids containing titanium dioxide, aluminum oxide, and copper nanoparticles in water under natural convection and radiation. The energy equation was numerically solved using the Runge-Kutta-Fehlberg method. Their graphical analysis detailed the effects of geometric and flow parameters on fin temperature distribution, emphasizing the enhanced heat transport capabilities of Cu-water nano liquid. Using ternary hybrid nanofluids, Suresh et al. [37] investigated thermal behavior in a dovetail fin under fully wet conditions. They considered temperature and humidity ratio differences as drivers for heat and mass transfer while analyzing surface convection, radiation, and internal heat generation effects. They solved the governing equation using the differential transformation method and the fourth-fifth order, the Runge-Kutta-Fehlberg (RKF) method. Their study emphasized ternary hybrid nanofluids' superior thermal response and dispersion characteristics. In conclusion, these advancements in fin technology enable the effective management of complex practical scenarios requiring rapid and substantial heat transfer. These innovations enhance thermal performance, allowing for swift and efficient handling of high heat loads. Such progress is crucial for applications needing quick heat dissipation to maintain optimal operational conditions, demonstrating notable achievements in this field.

Sowmya et al. [38] performed a transient analysis of porous fins using the finite difference method. They numerically determined the net heat transfer from the porous fin under transient conditions. Kheirandish et al. [39] analyzed solid fins with periodic base temperatures. They considered the non-Fourier heat conduction model and used the Spectral-Finite volume approach to perform the analysis. Yildirim et al. [40] determined thermal stresses in an annular fin with a time-dependent base temperature. They solved the governing equation using the Laplace

transformation method.Sahu and Bhowmick [41] numerically solved the composite fin with time-dependent boundary conditions using the lattice Boltzmann method and determined the temperature profile for various time-dependent boundary conditions. Ma et al. [42] performed a non-Fourier heat conduction analysis of a solid fin subjected to periodic base temperature. They used the element differential method to analyze and determine temperature distribution.

1.3 Aim of the Thesis

This thesis aims to study heat transfer properties for porous fins, especially in situations where the fin's base temperature changes over time, like in electronic devices and car engine blocks. For these applications to function optimally and prolong the life of the systems, effective and quick heat dissipation is necessary. For example, the heat produced in car engines must be quickly removed to avoid overheating and preserve engine efficiency. Similarly, reliable operation and prevention of thermal damage in electronic equipment depend on efficient heat management. Porous fins are advantageous in these situations because of their larger surface area, which improves heat transfer. Moreover, heat transmission can be greatly enhanced by adding nanofluid flow through porous fins. Furthermore, nanofluids have higher thermal conductivity than ordinary fluids, so heat transfer can be greatly enhanced by adding nanofluid flow through porous fins. However, there are several difficulties in researching heat transfer in porous fins with nanofluid flow due to the complexity of the governing equations, which include nonlinear terms. To complicate matters, the boundary conditions might also be periodic and frequently dependent on time. To properly represent the time-dependent aspect of the process, transient analysis is required, which means we have to solve a partial differential equation. Despite these obstacles, this thesis aims to close the current research gaps by creating and resolving the nonlinear partial differential equations with periodic boundary conditions representing the practical system and thoroughly examining the associated heat transfer mechanisms.

Chapter-2

2. PROBLEM FORMULATION AND SOLUTION

2.1 Problem Formulation

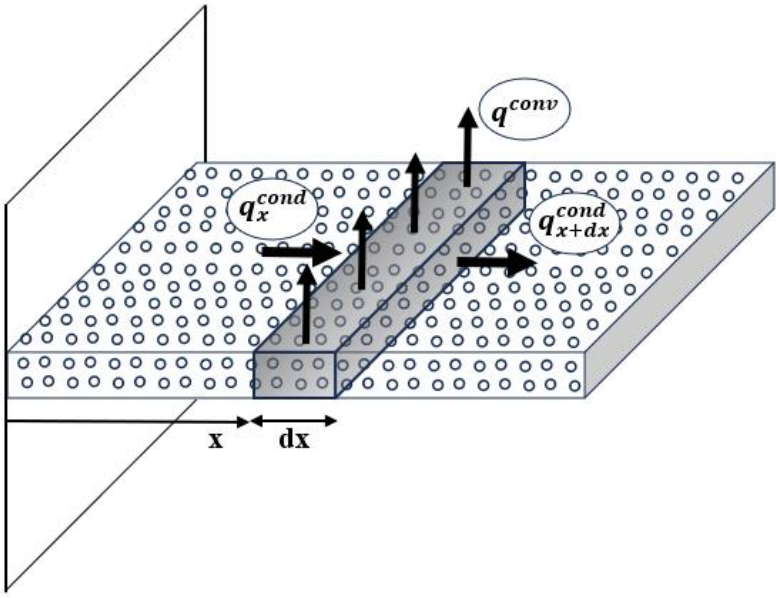

Fig.2.1 A schematic diagram of a longitudinal porous fin with a control volume for the energy balance.

Applying energy balance equation for a samall element length of dx we get

$$(q_x - q_{x+dx}) + q_{gen} w t_b dx - m c_{pf}(T - T_a) - 2hwdx(1-\varphi)(T - T_a) = [\rho c]_{eff} \frac{\partial T}{\partial t} w t_b dx \quad (2.1)$$

Applying Taylor's series expansion for the term q_{x+dx} we get

$$q_{x+dx} = q_x + \frac{\partial q_x}{\partial x} dx \quad (2.2)$$

Replacing q_{x+dx} term in governing equation

$$-\frac{\partial q_x}{\partial x} dx + q_{gen} w t_b dx - m c_{pf}(T - T_a) - 2hwdx(1-\varphi)(T - T_a) = [\rho c]_{eff} \frac{\partial T}{\partial t} w t_b dx \quad (2.3)$$

From Fourier's law of conduction

$$q_x = -k_{eff} w t_b \frac{\partial T}{\partial x} \quad (2.3)$$

Here effective thermal conductivity of the material is considered to account for the effects of porosity.

We are assuming effective thermal conductivity is independent of temperature

So,
$$-\frac{\partial}{\partial x}(-k_{eff} w t_b \frac{\partial T}{\partial x}) dx + q_{gen} w t_b dx - m c_{pf}(T - T_a) - 2hwdx(1-\varphi)(T - T_a) = [\rho c]_{eff} \frac{\partial T}{\partial t} w t_b dx \quad (2.4)$$

Or,
$$(k_{eff} w t_b \frac{\partial^2 T}{\partial x^2}) dx + q_{gen} w t_b dx - m c_{pf}(T - T_a) - 2hwdx(1-\varphi)(T - T_a) = [\rho c]_{eff} \frac{\partial T}{\partial t} w t_b dx \quad (2.5)$$

The expression for mass flow rate is given by

$$m = \rho_f v(x) w dx \tag{2.6}$$

Where expression for $v(x)$ is

$$v(x) = \frac{gK\beta_f \sin(\gamma)}{v_f}(T - T_a) \text{ [28]} \tag{2.7}$$

So, $$m = \frac{g\rho_f k_f \beta_f \sin(\gamma)}{v_f}(T - T_a) w dx \tag{2.8}$$

Replacing the expression for m in the governing equation we get

$$(k_{eff} w t_b \frac{\partial^2 T}{\partial x^2}) dx + q_{gen} w t_b dx - \frac{g\rho_f K \beta_f c_{pf} \sin(\gamma)}{v_f}(T - T_a)^2 w dx - 2hwdx(1 - \varphi)(T - T_a) = [\rho c]_{eff} \frac{\partial T}{\partial t} w t_b dx \tag{2.9}$$

By simplification we get

$$\frac{\partial^2 T}{\partial x^2} + \frac{q_{gen}}{k_{eff}} - \frac{g\rho_f K c_{pf} \sin(\gamma)}{v_f t_b k_{eff}}(T - T_a)^2 - \frac{2h(1-\varphi)}{t_b k_{eff}}(T - T_a) = \frac{[\rho c]_{eff}}{k_{eff}} \frac{\partial T}{\partial t} \tag{2.10}$$

Now nondimensionalizing the governing equation by putting

$X = \frac{x}{L}$; $\theta = \frac{T - T_a}{T_{bm} - T_a}$ and $\tau = \frac{t}{\frac{[\rho c]_{eff}}{k_{eff}} L^2}$

By substituting these our governing equation converted into

$$\frac{(T_{bm} - T_a)}{L^2} \frac{\partial^2 \theta}{\partial X^2} + \frac{q_{gen}}{k_{eff}} - \frac{g\rho_f K \beta_f c_{pf} \sin(\gamma)(T_{bm} - T_a)^2}{v_f t_b k_{eff}} \theta^2 - \frac{2h(1-\varphi)(T_{bm} - T_a)}{t_b k_{eff}} \theta = \frac{(T_{bm} - T_a)}{L^2} \frac{\partial \theta}{\partial \tau} \tag{2.11}$$

Or, $$\frac{\partial^2 \theta}{\partial X^2} + \frac{q_{gen} L^2}{k_{eff}(T_{bm} - T_a)} - \frac{g\rho_f K \beta_f c_{pf} \sin(\gamma)(T_{bm} - T_a) L^2}{v_f t_b k_{eff}} \theta^2 - \frac{2h(1-\varphi)L^2}{t_b k_{eff}} \theta = \frac{\partial \theta}{\partial \tau} \tag{2.12}$$

Let us assume that

$$A = \frac{g\rho_f K\beta_f c_{pf}\sin(\gamma)(T_{bm}-T_a)L^2}{\nu_f t_b k_{eff}}\ ;\ B = \frac{2h(1-\varphi)L^2}{t_b k_{eff}} \text{ and } C = \frac{q_{gen}L^2}{k_{eff}(T_{bm}-T_a)}$$

So, our governing equation converted into

$$\frac{\partial^2\theta}{\partial X^2} - A\theta^2 - B\theta + C = \frac{\partial\theta}{\partial\tau} \tag{2.13}$$

Equation (2.13) is a non-linear partial differential equation which is subjected to Periodic boundary condition at $X = 0$

$$\theta = 1 + \alpha\cos(\omega\tau) \tag{2.14}$$

Insulated tip boundary condition at $X = 1$

$$\frac{\partial\theta}{\partial x} = 0 \tag{2.15}$$

Initially the entire fin is at atmospheric temperature

$$\theta = \frac{T_a - T_a}{T_{bm} - T_a} = 0 \tag{2.16}$$

Therefore, at $\tau = 0$

$$\theta = 0 \tag{2.17}$$

2.2 Solution by Finite Difference Method

The governing equation we're dealing with is a nonlinear partial differential equation (PDE) characterized by its dependence on spatial and temporal variables. Additionally, the boundary conditions change over time, adding another layer of complexity. Nonlinear PDEs are inherently difficult to solve analytically because their solutions usually follow more complex methods. In our case, incorporating the effects of porosity into the equation introduces the nonlinear terms. This term complicates the behavior of the solution, making it hard to predict and manage through analytical techniques.

The analytical solution of our governing equation typically relies on simplifying assumptions or special techniques that only capture part of the problem's complexity, especially when dealing with nonlinearity and time dependency. Therefore, analytical solutions are limited to specific cases and may only be generalizable to some situations.

Given these challenges, a numerical solution becomes a more practical and effective approach. By applying finite difference method, we have successfully discretized the governing equation and boundary conditions into a form that can be handled computationally. This method can also accommodate the nonlinear nature of the PDE and the time-dependent boundary conditions more flexibly.

With this approach, we can simulate the system's behavior under various conditions and obtain approximate solutions that are sufficiently accurate for practical purposes. This approach enables us to handle the complexities and intricacies of the governing equation and its boundary conditions, providing valuable insights and results that would be difficult to achieve analytically.

To solve the governing equation numerically we have used finite difference method. As this method can efficiently handle the complexities of the governing equation and boundary conditions. Therefore, the governing equation of our problem without any undesired assumption is given by equation (2.13).

We have discretized all the terms and converted them into a set of algebraic equations to solve this nonlinear partial differential equation using the finite difference method. For discretization, we applied the Forward in Time and Central in Space (FTCS) scheme, which is second-order accurate in space and first-order accurate in time. Moreover, we have used the explicit method for discretizing the governing equation. In the explicit method, we use all the terms of the nth time step to calculate the terms in (n+1) th time step.

Discretizing the $\frac{\partial^2\theta}{\partial X^2}$ term by central difference

$$\frac{\partial^2\theta}{\partial X^2} \approx \frac{\theta_{j+1}^n - 2\theta_j^n + \theta_{j-1}^n}{(\Delta X)^2} \tag{2.18}$$

Where, j is spatial point and n is time step

Discretizing the term $\frac{\partial\theta}{\partial\tau}$ by forward difference

$$\frac{\partial\theta}{\partial\tau} \approx \frac{\theta_j^{n+1} - \theta_j^n}{\Delta\tau} \tag{2.19}$$

Substituting equations (2.18) and (2.19) into equation (2.13) we obtain

$$\frac{\theta_{j+1}^n - 2\theta_j^n + \theta_{j-1}^n}{(\Delta X)^2} - A\left(\theta_j^n\right)^2 - B\theta_j^n + C = \frac{\theta_j^{n+1} - \theta_j^n}{\Delta\tau} \tag{2.20}$$

By simplification we obtain

$$\theta_j^{n+1} = \theta_j^n + \Delta\tau\left[\frac{\theta_{j+1}^n - 2\theta_j^n + \theta_{j-1}^n}{(\Delta X)^2} - A\left(\theta_j^n\right)^2 - B\theta_j^n + C\right] \tag{2.21}$$

Now, Discretizing the boundary conditions

Boundary condition (2.14) converts into

At j=0,

$$\theta_0^n = 1 + \alpha\cos(\omega n\Delta\tau) \tag{2.22}$$

Boundary condition (2.15) converts into

At, $j = j_{max}$,

$$\frac{\theta^n_{j_{max}} - \theta^n_{j_{max}-1}}{\Delta X} = 0 \tag{2.23}$$

Or, $$\theta^n_{j_{max}} = \theta^n_{j_{max}-1} \tag{2.24}$$

Initial condition (2.17) converts into

At $n = 0$,

$$\theta^0_j = 0 \tag{2.25}$$

Now we can create a matrix having j_{max} number of column and n_{max} number of row and we can assign the initial condition and boundary conditions in that matrix and use Gauss Seidel method to calculate θ for all the value of i and n.

While selecting the step sizes, we must ensure that the FTCS scheme's stability criteria are satisfied and that smaller step sizes can provide accurate results.

2.3 Determining Heat Transfer Rate Through Fin

To determine the heat transfer rate through the fin, we have performed a control surface analysis. From the finite difference model, we can obtain non-dimensional temperature at various locations on the fin. Considering a small heat transfer surface around a point, we can easily calculate heat transfer from that surface by applying Newton's law of cooling. Finally, we added them to transfer heat from the entire surface.

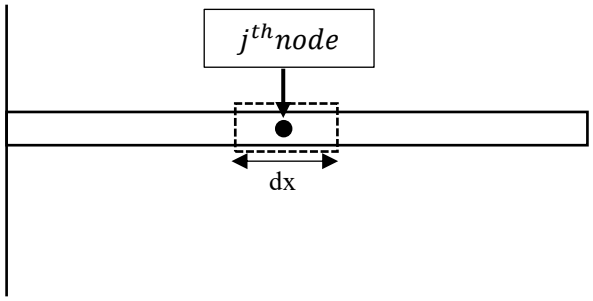

Fig. 2.2 A lattice point in a fin used in computational purpose.

For a significantly small value of dX, we can assume that the temperature remains constant within that small region.

Therefore, heat transfer rate through the small region is given by

$$dQ_j = dQ_j^{convection} + dQ_j^{nanofluid\ flow} \tag{2.26}$$

Or, $$dQ_j = 2hwdx(1-\varphi)(T-T_a) + \frac{g\rho_f K\beta_f c_{pf}\sin(\gamma)}{v_f}(T-T_a)^2 wdx \tag{2.27}$$

Again, from nondimensionalization conditions we know that

$X = \frac{x}{L}$ and $\theta = \frac{T-T_a}{T_{bm}-T_a}$ and by further simplification

Therefore, $$dQ_j = \frac{t_b k_{eff}(T_{bm}-T_a)\,wdX}{L}\left[A\theta_j^2 + B\theta_j\right] \tag{2.28}$$

Clearly, if we add dQ_j for all values of j then we can get the total heat transfer from the fin for a particular time.

2.4 Case Studies

2.4.1 Steady state solution by Adomian Decomposition method

If we look at our governing equation (2.13), we can see that it is a partial differential equation with a nonlinear term. The Adomian decomposition method is a well-established approach for addressing nonlinear terms. This method provides fast convergence only by considering a few terms in the series. Adomian decomposition method can provide an analytical solution by dealing with nonlinear terms. The result obtained by Adomian decomposition is well known for its high accuracy and close alignment with experimental studies. We have used this method to solve our governing equation under special conditions to check the accuracy of our numerical model. We have assumed a steady-state condition to solve this governing equation. Again, we must use a constant base temperature to achieve a steady state.

Our governing equation for steady state is

$$\frac{d^2\theta}{dX^2} - A\theta^2 - B\theta + C = 0 \tag{2.29}$$

Now the governing equation is subjected to modified boundary condition

Insulated tip condition at $X = 0$

$$\frac{d\theta}{dX} = 0 \tag{2.30}$$

Dirichlet boundary condition at $X = 1$

$$\theta = 1 \tag{2.31}$$

In Adomian decomposition method θ can be decomposed in an infinite series such as

$$\theta = \theta_0 + \theta_1 + \theta_2 + \theta_3 + \cdots \tag{2.32}$$

Adomian polynomial for θ^2 is given by

$$U(\theta) = \theta^2 = \sum_{N=0}^{\infty} P_N \tag{2.33}$$

Where, $P_N = \frac{1}{\mathrm{N!}} \times \left[\frac{d^N}{d\lambda^N} U\left(\sum_{\mathrm{J}=0}^{\infty} \lambda^J \theta_J\right)\right]_{\lambda=0}$ (2.34)

Therefore,

$$P_0 = \frac{1}{0!} \times \left[\frac{d^0}{d\lambda^0} U(\theta_0)\right]_{\lambda=0} \quad (2.35)$$

Or, $P_0 = U(\theta_0)$ (2.36)

Or, $P_0 = {\theta_0}^2$ (2.37)

Similarly,

$$P_1 = 2\theta_0\theta_1 \quad (2.38)$$

$$P_2 = {\theta_1}^2 + 2\theta_0\theta_2 \quad (2.39)$$

Let us assume,

$$\frac{d^2}{dX^2} = \Delta \quad (2.40)$$

and $\Delta^{-1} f(x) = \int_0^x \int_0^x f(u) du du$ (2.41)

Applying Adomian decomposition to our governing equation we get

$$\sum_{N=0}^{\infty} [\Delta\theta_N - AP_N - B\theta_N] + C = 0 \quad (2.42)$$

Or, $\sum_{N=0}^{\infty} [\Delta\theta_N] = \sum_{N=0}^{\infty} [AP_N + B\theta_N] - C$ (2.43)

Or, $\sum_{N=0}^{\infty} \theta_N = \sum_{N=0}^{\infty} \Delta^{-1}[AP_N + B\theta_N] - \Delta^{-1}C + \theta_{X=0} + X\frac{d\theta}{dX}_{X=0}$ (2.44)

Therefore,

$$\theta_0 = \theta_{X=0} + X\frac{d\theta}{dX}_{X=0} \quad (2.45)$$

Let us assume that temperature of fin tip is ξ

So, $\theta_0 = \xi$ (2.46)

Now, $\theta_1 = \Delta^{-1}[AP_0 + B\theta_0] - \Delta^{-1}C$ (2.47)

Or, $\theta_1 = \Delta^{-1}\left[A{\theta_0}^2 + B\theta_0\right] - \Delta^{-1}C$ (2.48)

Or, $\theta_1 = (A\xi^2 + B\xi - C)\frac{X^2}{2}$ (2.49)

Similarly,

$\theta_2 = \Delta^{-1}[AP_1 + B\theta_1]$ (2.51)

Or, $\theta_2 = \Delta^{-1}[A \times 2\theta_0\theta_1 + B\theta_1]$ (2.52)

Or, $\theta_2 = \Delta^{-1}\left[A \times 2\xi\left(\frac{A\xi^2X^2}{2} + \frac{B\xi X^2}{2} - \frac{CX^2}{2}\right) + B\left(\frac{A\xi^2X^2}{2} + \frac{B\xi X^2}{2} - \frac{CX^2}{2}\right)\right]$ (2.53)

Or, $\theta_2 = (2A\xi + B)(A\xi^2 + B\xi - C)\frac{A\xi^2X^4}{2\times3\times4}$ (2.54)

Again,

$\theta_3 = \Delta^{-1}[AP_2 + B\theta_2]$ (2.55)

Or, $\theta_3 = \Delta^{-1}[A({\theta_1}^2 + 2\theta_0\theta_2) + B\theta_2]$ (2.56)

Or, $\theta_3 = \Delta^{-1}\left[A\left\{(A\xi^2 + B\xi - C)\frac{X^2}{2}\right\}^2 + 2A\xi(A\xi^2 + B\xi - C)\frac{X^2}{2} + B(A\xi^2 + B\xi - C)\frac{X^2}{2}\right]$ (2.57)

Or, $\theta_3 = A(A\xi^2 + B\xi - C)^2\frac{X^6}{2\times2\times5\times6} + (2A\xi + B)(A\xi^2 + B\xi - C)\frac{X^4}{2\times3\times4}$ (2.58)

Therefore, the final expression for non-dimensional temperature is given by

$$\theta = \xi + (A\xi^2 + B\xi - C)\frac{X^2}{2} + (2A\xi + B)(A\xi^2 + B\xi - C)\frac{A\xi^2 X^4}{2\times3\times4} + (A\xi^2 + B\xi - C)^2\frac{X^6}{2\times2\times5\times6} + (2A\xi + B)(A\xi^2 + B\xi - C)\frac{X^4}{2\times3\times4} \quad (2.59)$$

The value of ξ falls between 0 and 1. To pinpoint the exact value of ξ, we have applied the boundary condition where X=1 and θ=1. By inserting this boundary condition into the equation, we have numerically solved for ξ. After finding the value of ξ, we have then substituted it into the final expression for θ, to accurately determine the temperature profile.

The analysis shows that the Adomian Decomposition Method offers several advantages, such as effectively handling non-linear terms and achieving rapid convergence with only a few terms. However, complexities arise when dealing with partial differential equations, especially when one of the boundary conditions is time-dependent. In such cases, the Laplace Transformation Method can be applied to address these complex situations and obtain transient analysis with periodic boundary conditions.

2.4.2 Solution by Laplace transformation method

As we have seen, our original governing equation contains a nonlinear term, but we know the Laplace transformation method cannot handle nonlinear terms. The Laplace transformation method is one of the most popular methods for solving partial differential equations, mainly when boundary condition depends on time. Therefore, with some assumptions, we have solved our governing equation with the Laplace transformation method and compared the result with our numerical model. The Laplace transformation method can provide an accurate analytical study of our governing equation with periodic base temperature boundary conditions. Applying the Laplace transformation converts the partial differential equation into an ordinary one. Hence, the dependent boundary condition is also converted into a constant boundary condition. That ordinary differential equation can be easily solved and finally by applying inverse Laplace transformation solution of the original partial differential equation can be obtained. To solve the equation using the Laplace transformation method, we neglected the nonlinear term of our original governing equation (2.13).

Therefore, our governing equation transformed into

$$\frac{\partial^2\theta}{\partial X^2} - B\theta + C = \frac{\partial\theta}{\partial\tau} \tag{2.59}$$

Now the governing equation is subjected to boundary condition given by equation number (2.14), insulated tip boundary condition given by equation number (2.15) and initial condition given by equation number (2.17)

Now applying Laplace transformation on both side equation (2.59)

$$\frac{d^2\bar{\theta}}{dX^2} - B\bar{\theta} + \frac{C}{s} = s\bar{\theta} - \theta_{\tau=0} \tag{2.60}$$

By applying initial condition (2.17) our equation coverts into

$$\frac{d^2\bar{\theta}}{dX^2} - B\bar{\theta} + \frac{C}{s} = s\bar{\theta} \tag{2.61}$$

Or, $$\frac{d^2\bar{\theta}}{dX^2} - (B+s)\bar{\theta} += -\frac{C}{s} \tag{2.62}$$

Applying Laplace transformation on the boundary conditions (2.14) and (2.15)

At, $X = 0$

$$\bar{\theta} = \frac{1}{s} + \frac{\alpha s}{s^2+\omega^2} \tag{2.63}$$

At, $X = 1$

$$\frac{d\bar{\theta}}{dX} = 0 \tag{2.64}$$

Our modified governing equation, given by (2.62), is a non-homogeneous ordinary differential equation. The solution to this equation includes both a complementary function and a particular integral.

Solving for complementary function

$$\frac{d^2\bar{\theta}}{dX^2} - (B+s)\bar{\theta} = 0 \tag{2.65}$$

Auxiliary equation is given by

$$[\psi^2 - (B+s)]\bar{\theta} = 0 \tag{2.66}$$

So, $\psi = \pm\sqrt{(B+s)}$

Therefore,

$$CF = \zeta_1 e^{(B+s)x} + \zeta_2 e^{-(B+s)x} \tag{2.67}$$

Solving for particular integral

$$PI = \frac{C}{s(B+s)} \tag{2.68}$$

The complete solution is given by

$$\bar{\theta} = CF + PI \tag{2.69}$$

$$\bar{\theta} = \zeta_1 e^{x\sqrt{(B+s)}} + \zeta_2 e^{-x\sqrt{(B+s)}} + \frac{C}{s(B+s)} \tag{2.70}$$

Applying boundary conditions (2.63) at $X = 0$

$$\bar{\theta}_{X=0} = \zeta_1 + \zeta_2 + \frac{C}{s(B+s)} \tag{2.71}$$

Or, $$\frac{1}{s} + \frac{\alpha s}{s^2+\omega^2} = \zeta_1 + \zeta_2 + \frac{C}{s(B+s)} \tag{2.72}$$

Or, $$\zeta_1 + \zeta_2 = \left(\frac{1}{s} + \frac{\alpha s}{s^2+\omega^2}\right) - \frac{C}{s(B+s)} \quad (2.73)$$

Applying boundary condition (2.64) at $X = 0$

$$\frac{d\bar{\theta}}{dX}_{X=1} = \zeta_1\sqrt{(B+s)}e^{\sqrt{(B+s)}} - \zeta_2\sqrt{(B+s)}e^{-\sqrt{(B+s)}} \quad (2.74)$$

Or, $$0 = \zeta_1\sqrt{(B+s)}e^{\sqrt{(B+s)}} - \zeta_2\sqrt{(B+s)}e^{-\sqrt{(B+s)}} \quad (2.75)$$

Or, $$\zeta_1 = \zeta_2 e^{-2\sqrt{(B+s)}} \quad (2.76)$$

Substituting the value of ζ_1 into equation (2.73) we get

$$\zeta_2 e^{-2\sqrt{(B+s)}} + \zeta_2 = \left(\frac{1}{s} + \frac{\alpha s}{s^2+\omega^2}\right) - \frac{C}{s(B+s)} \quad (2.77)$$

Or, $$\zeta_2 = \frac{e^{\sqrt{(B+s)}}}{(e^{-\sqrt{(B+s)}}+e^{\sqrt{(B+s)}})}\left(\frac{1}{s} + \frac{\alpha s}{s^2+\omega^2} - \frac{C}{s(B+s)}\right) \quad (2.78)$$

Form equation (2.73)

$$\zeta_1 = \frac{e^{-\sqrt{(B+s)}}}{(e^{-\sqrt{(B+s)}}+e^{\sqrt{(B+s)}})}\left(\frac{1}{s} + \frac{\alpha s}{s^2+\omega^2} - \frac{C}{s(B+s)}\right) \quad (2.79)$$

Therefore,

$$\bar{\theta} = \frac{e^{-\sqrt{(B+s)}}}{(e^{-\sqrt{(B+s)}}+e^{\sqrt{(B+s)}})}\left(\frac{1}{s} + \frac{\alpha s}{s^2+\omega^2} - \frac{C}{s(B+s)}\right)e^{x\sqrt{(B+s)}} + \frac{e^{\sqrt{(B+s)}}}{(e^{-\sqrt{(B+s)}}+e^{\sqrt{(B+s)}})}\left(\frac{1}{s} + \frac{\alpha s}{s^2+\omega^2} - \frac{C}{s(B+s)}\right)e^{-x\sqrt{(B+s)}} + \frac{C}{s(B+s)} \quad (2.80)$$

By further simplification

$$\bar{\theta} = \left(\frac{1}{s} + \frac{\alpha s}{s^2+\omega^2} - \frac{C}{s(B+s)}\right)\left[\frac{\cosh\left\{(x-1)\sqrt{(B+s)}\right\}}{\cosh\sqrt{(B+s)}}\right] + \frac{C}{s(B+s)} \quad (2.81)$$

Applying inverse Laplace transformation on each term

$$L^{-1}\left[\frac{\cosh\left\{(x-1)\sqrt{(B+s)}\right\}}{s\cosh\sqrt{(B+s)}}\right] = Sum\ of\ residues\ at\ poles \tag{2.82}$$

$\frac{\cosh\left\{(x-1)\sqrt{(B+s)}\right\}}{s\cosh\sqrt{(B+s)}}$ has simple poles at $s = 0$ and at $s = s_n$

Where, $s_n = -(2n-1)^2\left(\frac{\pi}{2}\right)^2 - B$ for $n = 1,2,3,4,5 \ldots\ldots$ (2.83)

Or, $\sqrt{(B+s_n)} = i\frac{\pi}{2}(2n-1)$ (2.84)

Residue at simple pole at is $s = 0$ given by

$$Residue_{s=0} = \lim_{s\to 0}\frac{(s-0)e^{s\tau}\cosh\left\{(x-1)\sqrt{(B+s)}\right\}}{s\cosh\sqrt{(B+s)}} \tag{2.85}$$

Or, $$Residue_{s=0} = \frac{\cosh\{(x-1)\sqrt{B}\}}{\cosh\sqrt{B}} \tag{2.86}$$

Residue at simple pole at is $s = s_n$given by

$$Residue_{s=s_n} = \lim_{s\to s_n}\frac{(s-s_n)e^{s\tau}\cosh\left\{(x-1)\sqrt{(B+s)}\right\}}{s\cosh\sqrt{(B+s)}} \tag{2.87}$$

Or, $$Residue_{s=s_n} = \lim_{s\to s_n}\frac{(s-s_n)}{\cosh\sqrt{(B+s)}} \times \lim_{s\to s_n}\frac{e^{s\tau}\cosh\left\{(x-1)\sqrt{(B+s)}\right\}}{s} \tag{2.88}$$

Here, $\lim_{s\to s_n}\frac{(s-s_n)}{\cosh\sqrt{(B+s)}}$ is in $\frac{0}{0}$ format therefore we can apply L'Hospital's rule

$$Residue_{s=s_n} = \lim_{s\to s_n}\frac{2\times\sqrt{(B+s)}}{\sinh\sqrt{(B+s)}} \times \lim_{s\to s_n}\frac{e^{s\tau}\cosh\left\{(x-1)\sqrt{(B+s)}\right\}}{s} \tag{2.89}$$

Or, $$Residue_{s=s_n} = \lim_{s\to s_n} \frac{(s-s_n)}{\cosh\sqrt{(B+s)}} \times \lim_{s\to s_n} \frac{e^{s\tau}\cosh\left\{(x-1)\sqrt{(B+s)}\right\}}{s} \quad (2.90)$$

Or, $$Residue_{s=s_n} = \frac{2\times\sqrt{(B+s_n)}}{\sinh\sqrt{(B+s_n)}} \times \frac{e^{s_n\tau}\cosh\{(x-1)\sqrt{(B+s_n)}\}}{s_n} \quad (2.91)$$

By substituting value of $\sqrt{(B+s_n)}$ from equation(2.84) we get

$$Residue_{s=s_n} = \frac{2\times i\frac{\pi}{2}(2n-1)}{\sinh\left\{i\frac{\pi}{2}(2n-1)\right\}} \times \frac{e^{s_n\tau}\cosh\left\{(x-1)i\frac{\pi}{2}(2n-1)\right\}}{s_n} \quad (2.92)$$

Now from the properties of hyperbolic functions we know that

$\cosh(i\emptyset) = \cos\emptyset$ and $\sinh(i\emptyset) = i\sin\emptyset$

Therefore,

$$Residue_{s=s_n} = \frac{2\times\frac{\pi}{2}(2n-1)}{\sin\left\{\frac{\pi}{2}(2n-1)\right\}} \times \frac{e^{s_n\tau}\cos\left\{(x-1)\frac{\pi}{2}\sqrt{(2n-1)}\right\}}{s_n} \quad (2.93)$$

We know that

$$\sin\left\{\frac{\pi}{2}(2n-1)\right\} = (-1)^{n+1} \quad (2.94)$$

So, $$Residue_{s=s_n} = (-1)^{n+1} \times \pi(2n-1) \times \frac{e^{s_n\tau}\cos\left\{(x-1)\frac{\pi}{2}(2n-1)\right\}}{s_n} \quad (2.95)$$

Therefore, from (2.82),(2.86) and (2.95) we get

$$L^{-1}\left[\frac{\cosh\left\{(x-1)\sqrt{(B+s)}\right\}}{s\cosh\sqrt{(B+s)}}\right] = \frac{\cosh\{(x-1)\sqrt{B}\}}{\cosh\sqrt{B}} + \sum_{n=1}^{\infty}(-1)^{n+1} \times \pi(2n-1) \times \frac{e^{s_n\tau}\cos\left\{(x-1)\frac{\pi}{2}(2n-1)\right\}}{s_n} \quad (2.96)$$

Similarly applying inverse Laplace transformation on the next term

$$L^{-1}\left[\left(\frac{\alpha s}{s^2+\omega^2}\right)\frac{\cosh\left\{(x-1)\sqrt{(B+s)}\right\}}{\cosh\sqrt{(B+s)}}\right] = \quad (2.97)$$
$$Sum\ of\ residues\ at\ poles$$

$\left(\frac{\alpha s}{s^2+\omega^2}\right)\frac{\cosh\left\{(x-1)\sqrt{(B+s)}\right\}}{\cosh\sqrt{(B+s)}}$ has poles at $s = i\omega, s = -i\omega$ and at $s = s_n$

where s_n is given by equation (2.83)

Similarly, residue at pole at is $s = i\omega$ given by

$$Residue_{s=i\omega} = \quad (2.98)$$
$$\lim_{s\to i\omega}(s - i\omega)\left(\frac{\alpha s}{s^2+\omega^2}\right)\frac{e^{s\tau}\cosh\left\{(x-1)\sqrt{(B+s)}\right\}}{\cosh\sqrt{(B+s)}}$$

Or,
$$Residue_{s=i\omega} = \left(\frac{\alpha}{2}\right)\frac{e^{i\omega\tau}\cosh\left\{(x-1)\sqrt{(B+i\omega)}\right\}}{\cosh\sqrt{(B+i\omega)}} \quad (2.99)$$

Again, residue at pole at is $s = -i\omega$ given by

$$Residue_{s=-i\omega} = \quad (2.100)$$
$$\lim_{s\to -i\omega}(s + i\omega)\left(\frac{\alpha s}{s^2+\omega^2}\right)\frac{e^{s\tau}\cosh\left\{(x-1)\sqrt{(B+s)}\right\}}{\cosh\sqrt{(B+s)}}$$

Or,
$$Residue_{s=-i\omega} = \left(\frac{\alpha}{2}\right)\frac{e^{-i\omega\tau}\cosh\left\{(x-1)\sqrt{(B-i\omega)}\right\}}{\cosh\sqrt{(B-i\omega)}} \quad (2.101)$$

Residue at simple pole at $s = s_n$ is given by

$$Residue_{s=s_n} = \quad (2.102)$$
$$\lim_{s\to s_n}(s - s_n)\left(\frac{\alpha s}{s^2+\omega^2}\right)\frac{e^{s\tau}\cosh\left\{(x-1)\sqrt{(B+s)}\right\}}{\cosh\sqrt{(B+s)}}$$

Or, $Residue_{s=s_n} = \lim_{s\to s_n} \frac{(s-s_n)}{\cosh\sqrt{(B+s)}} \times \lim_{s\to s_n} \left(\frac{\alpha s}{s^2+\omega^2}\right) e^{s\tau} \cosh\left\{(x-1)\sqrt{(B+s)}\right\}$ (2.103)

Previously we have calculated $\lim_{s\to s_n} \frac{(s-s_n)}{\cosh\sqrt{(B+s)}}$ so, once again repeating all those steps we get

$$Residue_{s=s_n} = (-1)^{n+1} \times \pi(2n-1) \times \left(\frac{\alpha s_n}{{s_n}^2+\omega^2}\right) e^{s_n\tau} \cos\left\{(x-1)\frac{\pi}{2}(2n-1)\right\} \quad (2.104)$$

From equations (2.97), (2.99), (2.101) and (2.104) we get

$$L^{-1}\left[\left(\frac{\alpha s}{s^2+\omega^2}\right)\frac{\cosh\left\{(x-1)\sqrt{(B+s)}\right\}}{\cosh\sqrt{(B+s)}}\right] = \left(\frac{\alpha}{2}\right)\frac{e^{i\omega\tau}\cosh\left\{(x-1)\sqrt{(B+i\omega)}\right\}}{\cosh\sqrt{(B+i\omega)}} + \left(\frac{\alpha}{2}\right)\frac{e^{-i\omega\tau}\cosh\left\{(x-1)\sqrt{(B-i\omega)}\right\}}{\cosh\sqrt{(B-i\omega)}} + \sum_{n=1}^{\infty}(-1)^{n+1} \times \pi(2n-1) \times \left(\frac{\alpha s_n}{{s_n}^2+\omega^2}\right) e^{s_n\tau} \cos\left\{(x-1)\frac{\pi}{2}(2n-1)\right\} \quad (2.105)$$

Now, applying inverse Laplace transformation on the next term

$$L^{-1}\left[\left\{\frac{C}{s(B+s)}\right\}\frac{\cosh\left\{(x-1)\sqrt{(B+s)}\right\}}{\cosh\sqrt{(B+s)}}\right] = Sum\ of\ residues\ at\ poles \quad (2.106)$$

$\left\{\frac{C}{s(B+s)}\right\}\frac{\cosh\left\{(x-1)\sqrt{(B+s)}\right\}}{\cosh\sqrt{(B+s)}}$ has poles at $s=0, s=-B$ and at $s=s_n$

where s_n is given by equation (2.83).

Residue at simple pole at $s=0$ is given by

$$Residue_{s=0} = \lim_{s\to 0} \frac{(s-0)e^{s\tau}\,\mathrm{C}\times\cosh\left\{(x-1)\sqrt{(B+s)}\right\}}{\mathrm{s(B+s)}\cosh\sqrt{(B+s)}} \quad (2.107)$$

Or, $$Residue_{s=0} = \frac{\mathrm{C}\times\cosh\{(x-1)\sqrt{B}\}}{\mathrm{B}\times\cosh\sqrt{B}} \quad (2.108)$$

Residue at simple pole at is $s = -B$ given by

$$Residue_{s=-B} = \lim_{s\to -B} \frac{(s+B)e^{s\tau}\,\mathrm{C}\times\cosh\left\{(x-1)\sqrt{(B+s)}\right\}}{\mathrm{s(B+s)}\cosh\sqrt{(B+s)}} \quad (2.109)$$

Or, $$Residue_{s=-B} = -\frac{\mathrm{C}\times e^{-B\tau}}{\mathrm{B}} \quad (2.110)$$

Residue at simple pole at $s = s_n$ is given by

$$Residue_{s=s_n} = \lim_{s\to s_n}(s-s_n)\left\{\frac{C}{s(B+s)}\right\}\frac{e^{s\tau}\cosh\left\{(x-1)\sqrt{(B+s)}\right\}}{\cosh\sqrt{(B+s)}} \quad (2.111)$$

Or, $$Residue_{s=s_n} = \lim_{s\to s_n}\frac{(s-s_n)}{\cosh\sqrt{(B+s)}} \times \lim_{s\to s_n}\left\{\frac{C}{s(B+s)}\right\}e^{s\tau}\cosh\left\{(x-1)\sqrt{(B+s)}\right\} \quad (2.112)$$

Previously we have calculated $\lim_{s\to s_n}\frac{(s-s_n)}{\cosh\sqrt{(B+s)}}$ so, once again repeating all those steps we get

$$Residue_{s=s_n} = (-1)^{n+1}\times\pi(2n-1)\times\left\{\frac{C}{s_n(B+s_n)}\right\}e^{s_n\tau}\cos\left\{(x-1)\frac{\pi}{2}(2n-1)\right\} \quad (2.113)$$

From equations (2.106), (2.108), (2.110) and (2.113) we get

$$L^{-1}\left[\left\{\frac{C}{s(B+s)}\right\}\frac{\cosh\left\{(x-1)\sqrt{(B+s)}\right\}}{\cosh\sqrt{(B+s)}}\right] = \frac{\mathrm{C}\times\cosh\{(x-1)\sqrt{B}\}}{\mathrm{B}\times\cosh\sqrt{B}} - \frac{\mathrm{C}\times e^{-B\tau}}{\mathrm{B}} + \sum_{n=1}^{\infty}(-1)^{n+1}\times\pi(2n-1)\times\left\{\frac{C}{s_n(B+s_n)}\right\}e^{s_n\tau}\cos\left\{(x-1)\frac{\pi}{2}(2n-1)\right\} \quad (2.114)$$

Now, applying inverse Laplace transformation on the last term

$$L^{-1}\left[\frac{C}{s(B+s)}\right] = Sum\ of\ residues\ at\ poles \tag{2.115}$$

$\frac{C}{s(B+s)}$ has simple poles at $s = 0\ and\ at\ s = -B$

Residue at simple pole at is $s = 0$ given by

$$Residue_{s=0} = \lim_{s\to 0} \frac{(s-0)e^{s\tau}\times C}{\mathrm{s(B+s)}} \tag{2.116}$$

Or, $$Residue_{s=0} = \frac{C}{\mathrm{B}} \tag{2.117}$$

Residue at simple pole at is $s = -B$ given by

$$Residue_{s=-B} = \lim_{s\to -B} \frac{(s+B)e^{s\tau}\times C}{\mathrm{s(B+s)}} \tag{2.118}$$

Or, $$Residue_{s=0} = -\frac{e^{-B\tau}C}{\mathrm{B}} \tag{2.119}$$

From equation (2.15), (2.17) and (2.19) we get

$$L^{-1}\left[\frac{C}{s(B+s)}\right] = \frac{C}{\mathrm{B}} - \frac{e^{-B\tau}C}{\mathrm{B}} \tag{2.120}$$

By considering all terms the final expression for non-dimensional temperature is given by

$$\theta = \frac{\cosh\{(x-1)\sqrt{B}\}}{\cosh\sqrt{B}} + \sum_{n=1}^{\infty}(-1)^{n+1} \times \pi(2n-1) \times \frac{e^{s_n\tau}\cos\left\{(x-1)\frac{\pi}{2}(2n-1)\right\}}{s_n} + \left(\frac{\alpha}{2}\right)\frac{e^{i\omega\tau}\cosh\left\{(x-1)\sqrt{(B+i\omega)}\right\}}{\cosh\sqrt{(B+i\omega)}} + \left(\frac{\alpha}{2}\right)\frac{e^{-i\omega\tau}\cosh\left\{(x-1)\sqrt{(B-i\omega)}\right\}}{\cosh\sqrt{(B-i\omega)}} + \sum_{n=1}^{\infty}(-1)^{n+1} \times \pi(2n-1) \times \left(\frac{\alpha s_n}{{s_n}^2+\omega^2}\right) e^{s_n\tau}\cos\left\{(x-1)\frac{\pi}{2}(2n-1)\right\} + \frac{\mathrm{C}\times\cosh\{(x-1)\sqrt{B}\}}{\mathrm{B}\times\cosh\sqrt{B}} - \frac{\mathrm{C}\times e^{-B\tau}}{\mathrm{B}} + \sum_{n=1}^{\infty}(-1)^{n+1} \times \pi(2n-1) \times \left\{\frac{C}{s_n(B+s_n)}\right\} e^{s_n\tau}\cos\left\{(x-1)\frac{\pi}{2}(2n-1)\right\} + \frac{C}{\mathrm{B}} - \frac{e^{-B\tau}C}{\mathrm{B}} \quad (2.121)$$

To determine the temperature profile, we have extracted the real part of the solution. This involves considering only the real component of the mathematical expression we obtain from solving the governing equation. By focusing on the real part, we can accurately represent the physical temperature distribution in the system. Although the Laplace transformation method can deal with time-dependent boundary conditions, it cannot handle the nonlinearity of the governing equation. However, to incorporate the effect of porosity, we must deal with nonlinear partial differential equations along with time-dependent boundary conditions. Due to these complexities, it is very difficult to get an analytical solution to the problem. In such cases, our numerical solution can efficiently handle the complexities of the governing equation and boundary condition. But Laplace transformation and Adomian decomposition methods solution helped us to check the validity and accuracy of our numerical model.

Chapter-3

3. RESULTS AND DISCUSSION

Before proceeding with any analysis, we must validate our numerical model to ensure its accuracy and reliability. Validation involves comparing the numerical model's results with known solutions to establish its credibility. In the "Case Studies" section of the previous chapter, we discussed two distinct analytical solution methods that will serve as benchmarks for our validation process.

Firstly, we explored the Adomian Decomposition Method (ADM) applied to the steady-state scenario. This method is particularly effective for solving nonlinear differential equations, making it suitable for our purposes. By comparing the numerical model's results with those obtained from the ADM, we validated the accuracy of the nonlinear term in our model. This comparison helped us confirm that our model correctly captures the system's nonlinear behavior under steady-state conditions. We have also validated our steady-state numerical solution with a published work.

Again, we examined a solution method using Laplace Transformation, simplifying the problem by neglecting the nonlinear term. This approach is useful for scenarios where the base temperature varies periodically. By validating our numerical model against the results derived from the Laplace Transformation method, we can ensure that our model accurately handles cases with periodic base temperature variations, even when nonlinear effects are not considered.

Together, these three validation steps, compared with the ADM and published work for steady-state nonlinear scenarios and with the Laplace Transformation solution for periodic base temperature scenarios, provide a comprehensive assessment of our numerical model's performance. This thorough validation process is crucial for establishing confidence in the model before using it for further analysis.

3.1 Steady State Validation with Adomian Decomposition

Firstly, we have validated our numerical model with the Adomian Decomposition Method (ADM) to the steady-state scenario. This method is particularly effective for solving nonlinear differential equations and is well-suited for our purposes. By comparing the results of our numerical model with those obtained from the ADM, we have validated the accuracy of the nonlinear term in our model. This comparison helped us confirm that our model accurately captures the system's nonlinear behavior under steady-state conditions. To perform this validation, we had to slightly modify our boundary conditions to match those of the Adomian decomposition solution. Specifically, we had to set $\alpha = 0$ in our numerical model, which converted our periodic base temperature condition into a constant base temperature condition. Additionally, we had to apply an insulated tip condition at $X = 0$ and a constant base temperature condition at $X = 1$ in our numerical model. By making these adjustments, we have compared the results of our numerical model with those obtained from the Adomian decomposition solution. To perform the validation, we have assumed A=2 , B=2 and C=2.

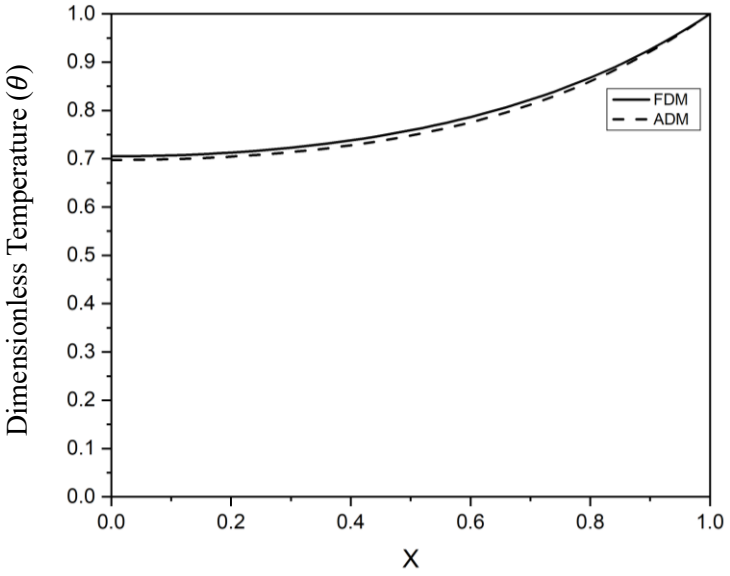

Figure 3.2: Steady state validation with ADM

Figure 3.1 clearly shows that the steady-state results of our numerical model align closely with those obtained using the Adomian Decomposition Method. This indicates that our numerical model effectively handles the nonlinearity of the governing equation. The close alignment between the steady-state results of our numerical model and the Adomian Decomposition Method demonstrates the robustness and accuracy of our approach. The Adomian Decomposition Method is known for its ability to solve nonlinear equations efficiently, so matching its results confirms that our numerical model can also tackle the complexities introduced by nonlinear terms in the governing equation. This validation provides confidence in the reliability of our numerical model for solving nonlinear problems.

3.2 Steady State Validation with Published Work

To enhance the reliability of our numerical model, we have validated our steady-state results against a published study. Roatamiyan et al. [38]. conducted a steady-state analysis of a porous fin in their paper titled "Analytical Investigation of Nonlinear Model Arising in Heat Transfer Through the Porous Fin." They employed the Variational Iteration Method to solve the steady-state nonlinear governing equations. For a meaningful comparison between our numerical model and their published results, we set the parameters in our model to A = 0.2, B = 1, and C = 0, as specified in their study. The resulting comparison graph is presented below, demonstrating the alignment between our numerical solutions and the analytical results obtained by Roatamiyan et al. [43].

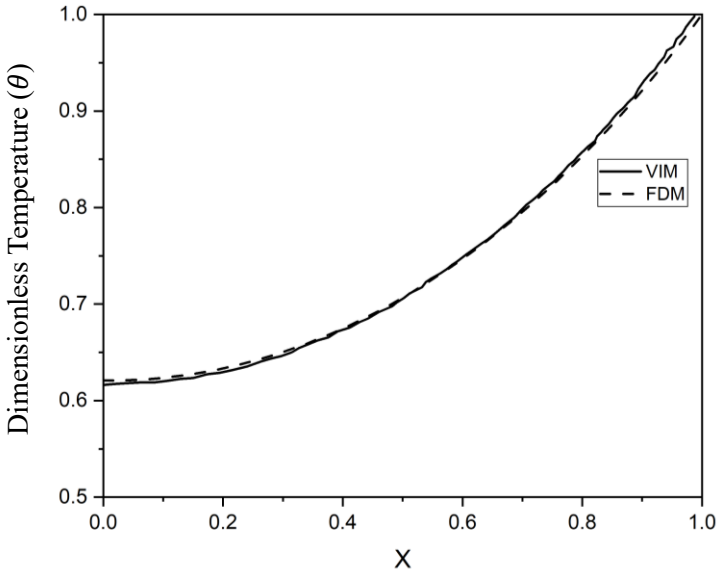

Figure 3.2 : Steady state validation with published work

From Fig. 3.2, we can clearly see that our numerical solution closely aligns with the published work.

3.3 Validation with Laplace Transformation

We have validated our numerical model by comparing it with the solution obtained using the Laplace Transformation method (Fig. 3.3). The Laplace Transformation simplifies the problem by neglecting the nonlinear term, making it particularly useful for scenarios where the base temperature varies periodically. By comparing our numerical model's results with those derived from the Laplace Transformation method, we can ensure the accuracy of our model in handling periodic base temperature variations. This validation process is crucial as it demonstrates that our model can accurately represent the system's behavior, confirming its reliability in every scenario. To perform the validation, we have taken $A = 0$,
$B = 0.15$, $C = 0.1$, $\alpha = 0.5$ and $\omega = 0.5$. We have plotted the temperature variation at $X = 0.5$ for various Fourier Number by using both method and compared those results.

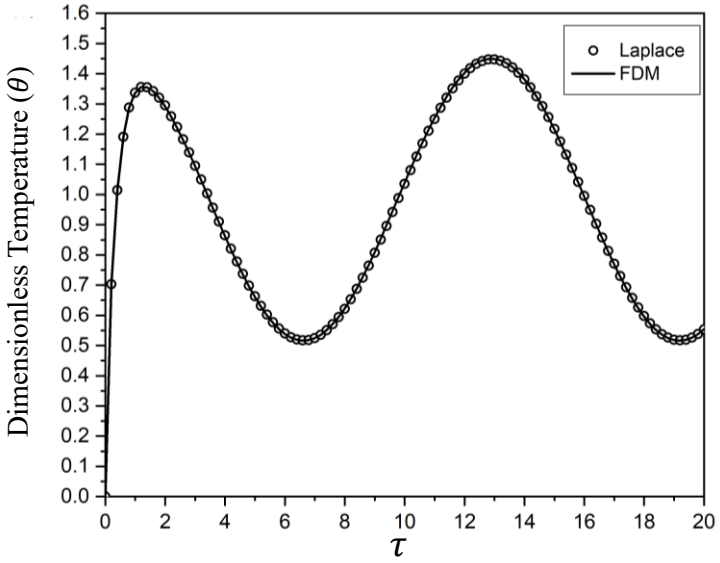

Figure 3.3: Validation with Laplace transformation

Figure 3.3 demonstrates that our numerical model aligns closely with the Laplace Transformation solution. This study indicates that our model

accurately captures the system's behavior under periodic base temperature variations.

With all three validations, we can conclude that our numerical model provides accurate solutions and is suitable for further analysis and discussion. The consistency of our model's predictions with the validation results demonstrates its reliability and effectiveness in capturing the key aspects of the heat transfer process through the porous fin. Consequently, we confidently proceed with more detailed investigations and apply our model to various scenarios for comprehensive understanding and insights.

3.4 Impact of Nano-Fluid Flow

In our study, we have used an Al_2O_3-water nanofluid with volume fraction 0.01 to enhance the heat transfer. Al_2O_3-water nanofluid is engineered colloidal suspensions of Al_2O_3 nanoparticles within base fluid water, have emerged as a promising solution for boosting heat transfer in various thermal management applications. Al_2O_3 nanoparticle is composed of metals oxides exhibit high thermal conductivity, which greatly improves the thermal performance of the base fluid. Nanoparticles increase thermal conductivity, enhance convection, and improve thermal dispersion, leading to more efficient heat transfer.

Properties of the Al_2O_3-water nanofluid can be evaluated with the empirical relations and property of Al_2O_3 nanoparticle described by Seth et al. [39]

Now, we have examined the temperature profile, heat transfer, and efficiency of a porous fin subjected to Al_2O_3-water nanofluid flow through its pores and a periodic base temperature. Using our numerical model, we have generated and analyzed the corresponding graphs to gain insights into the fin's thermal performance and behavior under these conditions.

First, we have determined the values of three arbitrary constants used in our analysis to plot the temperature profile. Expressions of those constants are given by

$$A = \frac{g\rho_f K\beta_f c_{pf}\sin(\gamma)(T_{bm}-T_a)L^2}{v_f t_b k_{eff}}\,;\; B = \frac{2h(1-\varphi)L^2}{t_b k_{eff}} \text{ and } C = \frac{q_{gen}L^2}{k_{eff}(T_{bm}-T_a)}$$

From, the book Drying Phenomena [41], we obtained the properties of water at ambient conditions and properties of the Al_2O_3-water nanofluid has evaluated with the empirical relations and property of Al_2O_3 nanoparticle described by Seth et al. [44]. Table 3.1 provides these properties.

Table 3.1: Properties of Water and Al_2O_3

	$\boldsymbol{\rho}\left(\frac{\boldsymbol{kg}}{\boldsymbol{m3}}\right)$	$\boldsymbol{c_p}\left(\frac{\boldsymbol{J}}{\boldsymbol{kgK}}\right)$	$\boldsymbol{k}\left(\frac{\boldsymbol{W}}{\boldsymbol{mK}}\right)$	$\boldsymbol{\beta}\left(\boldsymbol{K^{-1}}\right)$	$\boldsymbol{\mu}\,(\boldsymbol{Pas})$
Water [41]	995.7	4183	0.603	0.0003051	0.0007977
$\boldsymbol{Al_2O_3}$ [44]	3970	765	40	0.0000085	

From the analysis of Seth et al. [44], the expressions for nanofluid properties are given by

$$\rho_{nf} = (1-\epsilon)\rho_f + \rho_s \epsilon \tag{3.1}$$

$$\rho_{nf}\beta_{nf} = (1-\epsilon)\rho_f\beta_f + \epsilon\, \rho_s\beta_s \tag{3.2}$$

$$\rho_{nf}(c_p)_{nf} = (1-\epsilon)\rho_f(c_p)_f + \epsilon\, \rho_s(c_p)_s \tag{3.3}$$

$$k_{nf} = k_f \times \frac{k_s+2k_f-2\epsilon(k_f-k_s)}{k_s+2k_f+\epsilon(k_f-k_s)} \text{ [39]} \tag{3.4}$$

$$\mu_{nf} = \frac{\mu_f}{(1-\epsilon)^{2.5}} \tag{3.5}$$

Again,

$$k_{eff} = \varphi k_{nf} + (1-\varphi)k_{Al} \tag{3.6}$$

By substituting all these expressions, we get

$$A_{nf} = \left[\frac{gK(\rho_f c_{pf})(\rho_f \beta_f)\sin(\gamma)L^2(T_{bm}-T_a)}{\mu_f t_b}\right] \frac{\left[(1-\epsilon)+\frac{\epsilon\rho_s(c_p)_s}{\rho_f(c_p)_f}\right]\left[(1-\epsilon)+\frac{\epsilon\rho_s\beta_s}{\rho_f\beta_f}\right]}{\frac{1}{(1-\epsilon)^{2.5}}\times(k_{eff})_{nf}} \quad (3.7)$$

$$B_{nf} = \frac{2h(1-\varphi)L^2}{t_b(k_{eff})_{nf}} \quad (3.8)$$

$$C_{nf} = \frac{q_{gen}L^2}{(k_{eff})_{nf}(T_{bm}-T_a)} \quad (3.9)$$

Let us assume our fin is made of Aluminum having $k_{Al} = 237\frac{W}{mk}$ [45] and $L = 0.1m,\ w = 0.1m,\ t_b = 0.01m,\ (T_{bm} - T_a) = 50K,\ \sin\gamma = 1\ \ g = 9.81\frac{m^2}{s}$,$h = 100\frac{W}{m^2K}$,$q_{gen} = 1000\frac{W}{m^3}$,$\varphi = 0.2\ ,\ K = 2\times10^{-10}\frac{m}{s}\ ,\ \epsilon = 0.01$.

Now using these values, along with $\alpha = 0.5$ and $\omega = 0.5$ we have plotted the temperature profile of the fin and performed the further analysis.

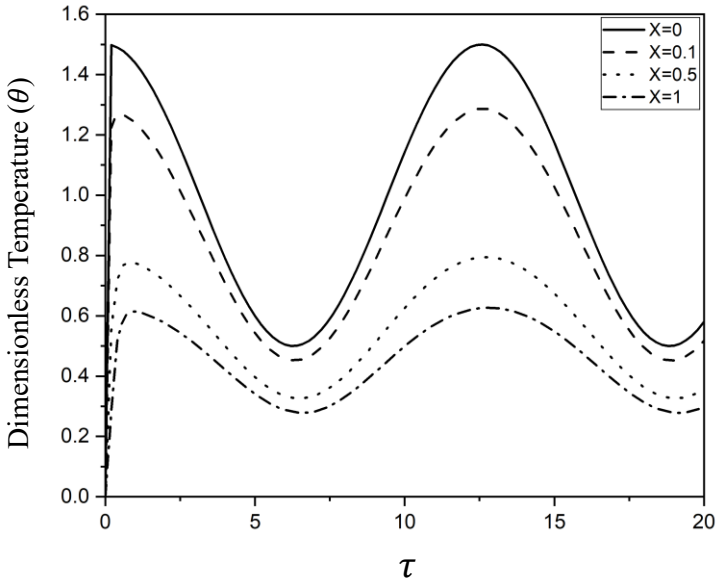

Figure 3.4.1: Non-dimensional temperature vs. Fourier number

In Fig. 3.4.1, we observe that for a given value of X, the non-dimensional temperature varies periodically with the Fourier number (or non-dimensional time). At X=0, the base temperature of the fin is perfectly following the induced periodic boundary condition. Additionally, as the value of X increases, meaning as the distance from the fin base increases, the maximum temperature value decreases. This is due to the nanofluid flow through the pores and the convection occurring between the fin and its surroundings, which results in heat loss and consequently lowers the maximum temperature.

To better understand this phenomenon, we have plotted the non-dimensional temperature against X for a specific Fourier number as shown in Fig. 3.4.2. This would illustrate how the temperature distribution changes along the length of the fin at a particular moment in time.

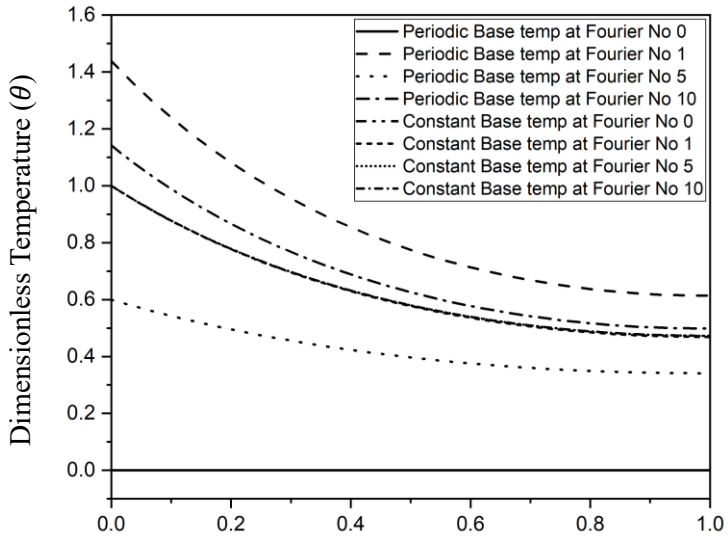

Figure 3.4.2: Non-dimensional temperature vs X at various Fourier number.

From Fig. 3.4.2 for non-dimensional temperature versus X for a specific Fourier number, we can clearly observe that the temperature decreases as X increases. This trend is due to heat loss through convection and the cooling

effect of nanofluid flow through the porous fin. As the distance from the fin base increases, the heat dissipates more, leading to a lower temperature.

Moreover, we can see that the base of the fin varies periodically with the non-dimensional time or Fourier number. This periodic variation results from the boundary conditions of our problem, where the base temperature is influenced by external factors, causing it to fluctuate over time. This periodic behavior at the base sets the stage for the observed temperature profile along the fin's length. In addition, the condition of constant base temperature has been plotted for various Fourier numbers. We can observe that the fin achieves a steady state with a constant base temperature.

By examining these graphs, we better understand how heat is transferred and dissipated along the fin. They highlight the impacts of convection, fluid flow, and boundary conditions on the fin's thermal performance.

We have performed some more calculations to determine the heat transfer from the fin. We have already derived the equation for heat transfer through a small control surface in equation (2.28).

By substituting values of all constants, along with $dX = 0.02$ we have determined dQ_i and total heat transfer through fin is given by $\sum_{i=0}^{i=i_{max}} dQ_i$. Therefore, by using that we have plotted the heat transfer for various Fourier numbers.

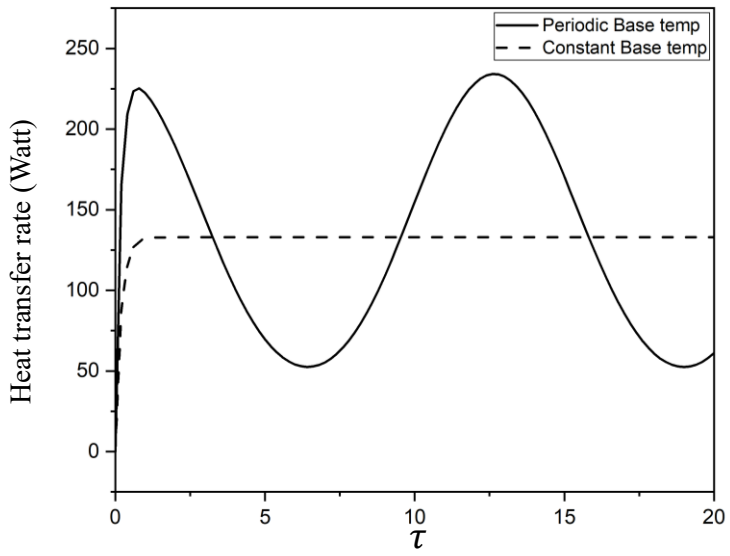

Figure 3.4.3: Heat transfer rate vs Fourier number

From Fig. 3.4.3 for heat transfer versus Fourier number (non-dimensional time), it is evident that in porous fin with periodic base temperature condition the heat transfer rate exhibits a periodic variation, mirroring the fin base temperature variation. This periodicity indicates that as the base temperature of the fin varies cyclically, the rate at which heat is transferred also follows a similar cyclical pattern. A closer inspection of the graph reveals an interesting observation: the peak value of heat transfer during the first cycle is slightly lower than that of the second. This phenomenon occurs because the entire fin is initially at ambient temperature. At the start, the fin requires time to absorb heat and develop a temperature gradient along its length, which is essential for effective heat transfer. As the fin gradually heats up, it establishes a temperature profile, allowing for an increase in heat transfer rate. Therefore, the heat transfer is lower during the first cycle than in subsequent cycles. Once the fin has gone through the first cycle, it no longer starts from the ambient temperature but rather from a higher initial temperature closer to the periodic base temperature. This allows the fin to achieve higher heat transfer rates more quickly in subsequent cycles, resulting in higher peak values. Thus, the graph shows the periodic nature of heat transfer and highlights the initial lag in heat transfer efficiency due

to the starting ambient conditions. In the other plot of porous fins with a constant base temperature, the heat transfer rate gradually achieves a steady state.

To evaluate the enhancement in heat transfer achieved by introducing a porous fin with nanofluid flow, we have compared it with a porous fin with water (base fluid) flow and a solid fin under similar conditions. By determining the temperature profile and heat transfer rate for the porous fin with water flow and solid fin, we have effectively compared all the results and gained insights into the thermal performance improvement provided by the porous fin with nanofluid flow.

To plot the temperature profile for porous fin with water flow and solid fin we have determined the values of three arbitrary constants A, B and C used in our analysis by using table (3.1) for values of properties and equation (3.6) to determine k_{eff}. For solid fin $A = 0$ and $\varphi = 0$ so, $k_{eff} = k_{Al}$. We have considered all of the other parameters similar to the analysis of porous fin with nanofluid flow to have a proper comparison.

Now, by substituting all, we have plotted the temperature profile of the solid fin, porous fin with base fluid flow, and porous fin with nanofluid flow and compared the result with the porous fin with nanofluid flow as depicted in Figs. 3.4.4 and 3.4.5.

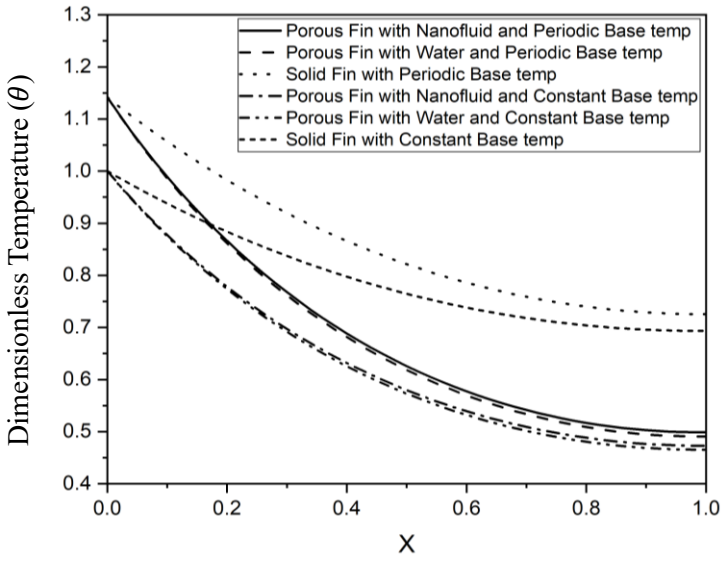

Figure 3.4.4: Non-dimensional temperature vs X Comparison for Fourier number 10.

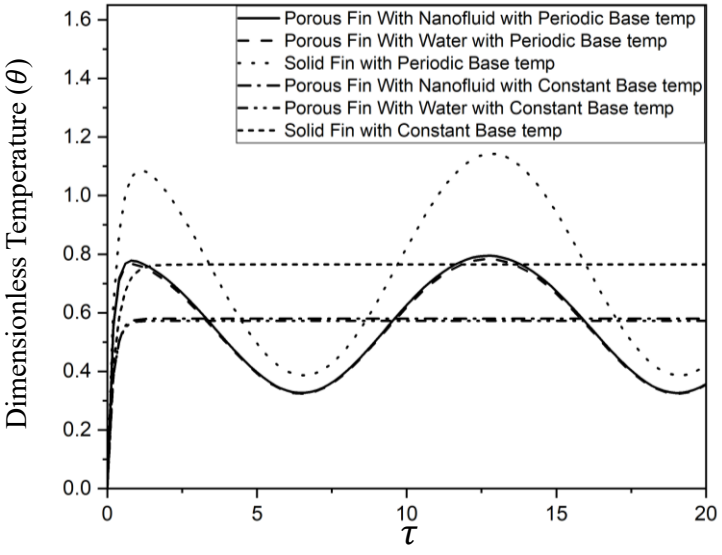

Figure 3.4.5: Non-dimensional temperature vs Fourier number Comparison at X=0.5

From analyzing these two graphs above, it becomes clear that the porous fin maintains a considerably lower temperature than the solid fin under the same conditions. This is primarily because the porous fin's structure offers a much larger surface area, which significantly enhances heat dissipation. The increased surface area allows for more efficient thermal exchange between the fin and its surroundings. Furthermore, introducing Al2O3-water nanofluid in the porous fin increases heat transfer. As Al2O3-water nanofluids have higher thermal conductivity compared to conventional fluids, which means they can carry heat away from the fin more effectively, but in Al2O3 nanofluid, nanoparticles absorb some amount of heat, which results in the porous fin with Al2O3-water nanofluid flow operating at a higher temperature than the solid fin and porous fin with water flow. Due to this, the temperature difference between the fin and surrounding is slightly higher, causing higher convection in porous fin with nanofluid than porous fin with water. We can also observe that a fin with a constant base temperature gradually achieves a steady state. Still, a fin with a periodic base temperature follows the periodic temperature pattern with an increasing Fourier number.

We performed some more calculations to determine the heat transfer from the solid fin and porous fin with water flow. We have already derived the equation for heat transfer through a small control surface. By substituting values of all constants, we have plotted the heat transfer in solid fin and porous fin with water flow for various Fourier numbers and compare that with the heat transfer from porous fin with nanofluid flow shown in Fig. 3.4.6.

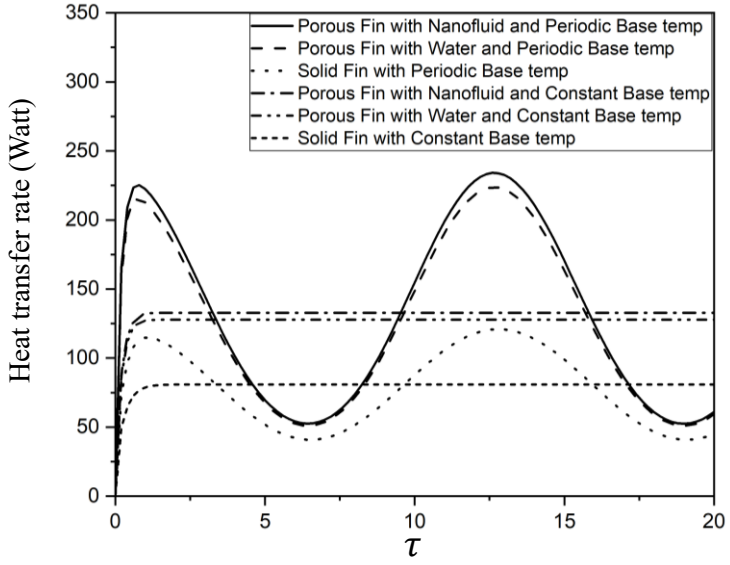

Figure 3.4.6: Heat transfer rate vs Fourier number comparison.

Table 3.2: Heat transfer rate vs Fourier number comparison

Fourier Number	Heat transfer in Solid Fin with Periodic Base temp (Watt)	Heat transfer in Solid Fin with Constant Base temp (Watt)	Heat transfer in Porous Fin with Water and Periodic Base temp (Watt)	Heat transfer in Porous Fin with Water and Constant Base temp (Watt)	Heat transfer in Porous Fin with Nanofluid and Periodic Base temp (Watt)	Heat transfer in Porous Fin with Nanofluid and Periodic Base temp (Watt)
1	114.781	78.731	212.672	127.126	222.454	132.145
2	106.134	80.806	181.291	127.739	189.416	132.853
3	88.292	80.878	138.574	127.739	144.385	132.853
4	68.531	80.879	97.4978	127.739	101.180	132.853
5	51.791	80.879	67.403	127.739	69.626	132.853
6	42.173	80.879	52.492	127.739	54.028	132.853
7	42.032	80.879	53.704	127.739	55.249	132.853
8	51.402	80.879	71.524	127.739	73.799	132.853
9	67.991	80.879	105.073	127.739	108.912	132.853
10	87.735	80.879	148.552	127.739	154.639	132.853

Fig. 3.4.6 and Table 3.2 clearly demonstrate that a porous fin with Al_2O_3 water nanofluid flow significantly enhances heat transfer compared to a solid fin and substantially improves it compared to a porous fin with water flow. In this study, we used a nanofluid volume fraction of only 0.01, which already shows an enhancement in heat transfer. Increasing the volume fraction of nanoparticles could potentially enhance heat transfer even further. The study confirms that incorporating a porous fin improves heat transfer in practical situations, and this enhancement can be amplified by using nanofluid flow. Again, from Fig. 3.4.6 and Table 3.2, we can see that fins with constant base temperatures achieve a steady heat transfer rate after some time, but fins with periodic base temperatures follow a periodic variation of heat transfer rate and never achieve a steady state.

Chapter-4

4. FUTURE SCOPE AND CONCLUSION

4.1 Future scope

This thesis studies porous fins with periodic base temperature and nanofluid flow. Along with the main numerical solution model, a steady-state solution was obtained using the Adomian Decomposition Method, and the periodic base temperature solution was derived through Laplace transformation while neglecting nonlinear terms. The future scope of this research includes several promising directions:

Combining Solution Methods:

Integration of the Adomian Decomposition Method and Laplace transformation to solve the nonlinear PDE with time-dependent boundary conditions might be possible. By utilizing the Laplace transformation, nonlinear PDE can be converted into a nonlinear ODE, and then the Adomian Decomposition Method can be applied to solve the nonlinear ODE. Finally, by performing the inverse Laplace transformation, the analytical solution of the entire governing equation without any unnecessary assumptions might be possible.

Improving Numerical Accuracy:

Applying other discretization schemes, such as the central-in-time central-in-space scheme or the Crank-Nicolson scheme, might improve the accuracy of the current finite difference method.

Optimizing the step size to improve the precision of the solution might be possible.

Exploring Different Nanofluids:

It might be possible to investigate different nanofluids beyond the Al2O3-water nanofluid considered in this study to further enhance heat transfer.

Examining the impact of nanoparticle volume fraction enhancement through geometric modifications of nanoparticles might be possible.

Advanced Nanofluid Configurations:

Exploring the potential of hybrid nanofluids and ternary hybrid nanofluids to achieve superior heat transfer characteristics might be possible.

Considering the strategic use of magnetic nanofluids, which can be precisely manipulated using Lorentz forces to significantly boost heat transfer efficiency, is a technical avenue worth exploring.

By pursuing these avenues, the scope of the research can be significantly broadened, leading to more comprehensive and effective heat transfer solutions in practical applications.

4.2 Conclusion

This thesis thoroughly investigates heat transfer dynamics within porous fins infused with nanofluids under time-dependent base temperature conditions. The study employs a numerical model based on the finite volume method with the explicit FTCS scheme to simulate heat transfer phenomena. An analytical solution using Laplace transformation, which neglects nonlinear terms, complements the numerical findings. Furthermore, the Adomian Decomposition Method validates nonlinear terms under steady-state conditions with a constant base temperature.

This research underscores the practical implications of porous media with Al2O3-water nanofluids flow in augmenting heat transfer, a significant departure from the conventional solid fin and porous fin with water flow. The insights offered here have the potential to significantly

impact the practical applications in the field of thermal management. The numerical analyses delve into the influence of nanofluid properties on heat transfer rates, thereby opening up opportunities for optimizing thermal performance in various engineering applications.

In conclusion, this thesis comprehensively analyzes heat transfer augmentation in Al2O3-water nanofluid-infused porous fins under dynamic thermal conditions. By integrating numerical and analytical approaches, the study contributes insights that could enhance the design and efficiency of fins for advanced thermal management systems.

Chapter-5

5. REFERENCES

[1] D. R. Harper and W. B. Brown, "Mathematical equations for heat conduction in the fins of air cooled engines," NACA, 1922.

[2] K. A. Gradner, "Efficiency of extended surface," 1945.

[3] H. S. Carslaw and J. C. Jaeger, Conduction of Heat in Solids, Oxford: Clarendon Press, 1959.

[4] M. H. Cobble, "Nonlinear fin heat transfer," *Journal of the Franklin Institute,* vol. 277, pp. 206-216, 1964.

[5] M. H. Cobble, "Optimum fin shape," *Journal of the Franklin Institute,* vol. 291, pp. 283-292, 1971.

[6] M. N. Ozisik, Heat Conduction, Wiley, 1980.

[7] W. S. Minkler and W. T. Rouleau, "The Effects of Internal Heat Generation on Heat Transfer in Thin Fins," *Nuclear Science and Engineering ,* vol. 7, 1960.

[8] W. V. Chen and B. J. Fulker, " Heat transfer in composite circular fins," in *International heat transfer conference*, Tokyo, 1974.

[9] M. A. Heaslet and H. Lomax, "Numerical predictions of radiative interchange between conducting fins with mutual irradiations," NASA, 1961.

[10] M. Cumo, S. Lopez and Pinchera, "Numerical calculation of extended surface efficiency," *Chemical Engineering Progress,* vol. 61, 1965.

[11] H. M. Hung and F. C. Appl, "Heat Transfer of Thin Fins With Temperature-Dependent Thermal Properties and Internal Heat Generation," *Journal of heat transfer,* vol. 89, pp. 155-162, 1967.

[12] N. K. Sane and S. P. Sukhatme, "Natural convection heat transfer from horizontal rectangular fin arrays," in *International heat transfer conference*, Tokyo, 1974.

[13] A. Campo, "Variational techniques applied to radiative-convective fins with steady and unsteady conditions," *Wärme- und Stoffübertragung,* vol. 9, p. 139–144, 1976.

[14] E. M. Sparrow and C. F. Hsu, "Analytically determined fin-tip heat transfer coefficients," *Journal of Heat Transfer,* vol. 103, pp. 18-25, 1981.

[15] M.-I. Char and C.-K. Chen, "Transient thermal response of a composite trapezoidal fin assembly," *Journal of the Chinese Society of Mechanical Engineers,* vol. 6, pp. 27-33, 1985.

[16] A. J. Chapman, "Transient heat conduction in annular fins of uniform thickness," in *ASME-AIChe heat transfer conference*, Chicago, 1958.

[17] A. B. Donaldson and A. R. Shouman, "Unsteady state temperature distribution in a convecting fin of constant area," *Applied Scientific Research ,* vol. 26, pp. 75-85, 1972.

[18] C. W. Bert, "Nonsymmetric temperature distributions in varying thickness circular," *Journal of heat transfer,* vol. 85, pp. 77-78, 1963.

[19] K. N. Newhouse, " Temperature distributions in circular fins of rectangular profile," *Journal of heat transfer,* vol. 86, pp. 563-564, 1964.

[20] N. I. Malikov, " Influence of tangential heat transfer in the thermal condition of a ribbed cylinder," *Machinostroene ,* 1966.

[21] E. M. Sparrow and D. K. Hennecke, " Temperature depression at the base of a fin," *Journal of heat transfer,* vol. 92, pp. 204-206, 1970.

[22] J. W. Yang, "Periodic heat transfer in straight fins," *Journal of heat transfer,* vol. 94, pp. 310-314, 1972.

[23] A. Aziz, "Periodic heat transfer in annular fins," *Journal of heat transfer,* vol. 97, pp. 302-303, 1975.

[24] E. M. Sparrow and L. Lee, "Effects of Fin Base-Temperature Depression in a Multifin Array," *Journal of heat transfer,* vol. 97, pp. 463-465, 1975.

[25] A. Aziz and T. Y. Na, "Perturbation analysis for periodic heat transfer in radiating fins," *Heat and mass transfer,* 1981.

[26] A. Mujahid, "Periodic Heat Transfer in Triangular Fins," *Journal of Heat and Technology,* vol. 3, pp. 61-81, 1985.

[27] H. Darcy, Les fontaines publiques de la ville de Dijon, 1856.

[28] A. Bejan and D. A. Nield, Convection in Porous Media, Springer, 1992.

[29] M. Kaviany, Principles of Heat Transfer in Porous Media, Springer, 1995.

[30] S. Y. Kim and A. Mem, "Flow and Heat Transfer Correlations for Porous Fin in a Plate-Fin Heat Exchanger," *Journal of Heat Transfer,* vol. 122, no. 3, pp. 572-578, 2000.

[31] B. Kundu and D. Bhanja, "An analytical prediction for performance and optimum design analysis of porous fins,"

International Journal of Refrigeration, vol. 34, no. 1, pp. 337-352, 2011.

[32] M. G. Sobamowo, A. A. Yinusa, M. O. Salami, O. C. Osih and B. O. Adesoye, "Heat Transfer Analysis of a Rectangular Moving Porous Fin with Temperature-Dependent Thermal Conductivity and Internal Heat Generation: Comparative and Parametric Studies," *Engineering Advances,* vol. 1, no. 2, pp. 50-66, 2021.

[33] M. Ghazvini and H. Shokouhmand, "Investigation of a nanofluid-cooled microchannel heat sink using Fin and porous media approaches," *Energy Conversion and Management,* vol. 50, no. 9, pp. 2373-2380, 2009.

[34] S. G., G. B.J. and P. B.C., "Scrutinization of different shaped nanoparticle of molybdenum disulfide suspended nanofluid flow over a radial porous fin," *International Journal of Numerical Methods for Heat & Fluid Flow,* vol. 30, no. 7, pp. 3685-3699, 2020.

[35] G. Manohar, P. Venkatesh, B. Gireesha, J. Madhukesh and G. Ramesh, "Dynamics of hybrid nanofluid through a semi spherical porous fin with internal heat generation," *Partial Differential Equations in Applied Mathematics,* vol. 4, 2021.

[36] G. S. Abeer Baslem, B. Gireesha, B. Prasannakumara, M. Rahimi-Gorji and N. M. Hoang, "Analysis of thermal behavior of a porous fin fully wetted with nanofluids: convection and radiation," *Journal of Molecular Liquids,* vol. 307, 2020.

[37] J. S. Goud, P. Srilatha, R. V. Kumar, K. T. Kumar, U. Khan, Z. Raizah, H. S. Gill and A. M. Galal, "Role of ternary hybrid nanofluid in the thermal distribution of a dovetail fin with the internal generation of heat," *Case Studies in Thermal Engineering,* vol. 35, 2022.

[38] G. Sowmya, B. J. Gireesha and H. Berrehal, “An unsteady ıal investigation of a wetted longitudinal porous fin of different

es," *Journal of Thermal Analysis and Calorimetry,* vol. 143, p. –2474, 2020. vol. 143, p. 2463–2474, 2020.

[39] Z. Kheirandish, M. Kharati-Koopaee and A. Omidvar, "Numerical study into the fin performance subjected to different periodic base temperatures employing Fourier and non-Fourier heat conduction models," *International Communications in Heat and Mass Transfer,* vol. 114, 2020.

[40] A. Yildirim, D. Yarimpabuç and K. Celebi, "Transient thermal stress analysis of functionally," *Journal of Thermal Stresses,* pp. 1-12, 2020.

[41] A. Sahu and S. Bhowmick, "Continuous composite longitudinal fins under oscillating boundary conditions: a lattice Boltzmann solution," *Engineering Computations,* 2024.

[42] J. Ma, Y. Sun and S. Li, "Element Differential Method for Non-Fourier Heat Conduction in the Convective-Radiative Fin with Mixed Boundary Conditions," *Coatings,* vol. 12, 2022.

[43] Y. ROSTAMIYAN, D. D. GANJI, I. R. PETROUDI and M. K. NEJAD, "Analytical Investigation of Non-Linear Model Arising in Heat Transfer Through the Porous Fin," *Thermal Science,* vol. 18, no. 2, pp. 409-417, 2014.

[44] G. S. Seth, R. Kumar and R. Tripathi, "Thermo-diffusion effects on the magnetohydrodynamic natural convection flow of a chemically reactive Brinkman type nanofluid in a porous medium," *Bulgarian Chemical Communications,* vol. 51, no. 1, pp. 168 - 179, 2019.

[45] İ. Dinçer and C. Zamfirescu, "Thermophysical Properties of Water," in *Drying Phenomena*, John Wiley & Sons, Ltd., 2016, pp. 457 - 459.